Supporting Information

Thiacalixarene-supported $M_{20}V_8$ (M = Fe, Co, Ni) square pyramid nanocages for visible light photothermal catalysis

Qiqi Li,[a] Yuhan Zou,[a] Dongao Mao, Hongrui Tian,[a] Xinxin Hang*[b] and Yanfeng Bi*[a]

[a] *School of Petrochemical Engineering, Liaoning Petrochemical University, Fushun 113001, P. R. China. E-mail: biyanfeng@lnpu.edu.cn*

[b] *Institute for Innovative Materials and Energy, School of Chemistry and Chemical Engineering, Yangzhou University, Yangzhou, Jiangsu 225002, P. R. China. E-mail: hangxinxin@yzu.edu.cn*

Experimental section

Materials and Measurements

p-tert-Butylthiacalix[4]arene (H$_4$TC4A) was synthesized according to a previously reported method.[1] Other chemicals were purchased from commercial sources and used as received without further purification. Powder X-ray diffraction (PXRD) patterns were collected on a Bruker D8 VENTURE diffractometer with Cu-Kα radiation. Fourier transform infrared (FT-IR) spectra using KBr pellets were obtained using a PerkinElmer Spectrum GX spectrometer. Thermogravimetric analysis (TGA) was performed on a TAQ600 thermogravimetric analyzer. Elemental analyses (C, H, and N) were performed on a EuroVector EA3000 elemental analyzer. X-ray photoelectron spectroscopic (XPS) measurements were carried out on an ESCALAB 250Xi using a monochromic Al Kα X-ray source (1486.6eV). The solid and solution ultraviolet-visible (UV-vis) spectra were recorded using an Agilent Cary5000 spectrometer.

Synthesis of {H[Fe$_{20}$(TC4A)$_5$(Cl)$_5$(CH$_3$CH$_2$VO$_4$)$_8$] (+solvents)} (Fe$_{20}$V$_8$)

Fe$_{20}$V$_8$ was obtained from solvothermal reaction of the mixture of H$_4$TC4A (0.1 mmol, 72 mg), FeCl$_2$·4H$_2$O (0.4 mmol, 80 mg), Na$_3$VO$_4$·12H$_2$O (0.16 mmol, 60 mg), N, N-dimethylformamide (DMF, 5.0 mL), and ethanol (CH$_3$CH$_2$OH, 5.0 mL) in a Teflon-lined autoclave (20 mL), which was kept at 130 °C for 72 h and then slowly cooled to 20 °C at approximately 4 °C h^{-1}. Black long-strip crystals were isolated by filtration, washed with CH$_3$CH$_2$OH, and dried in air. Yield: 55.9 % (based on H$_4$TC4A). Elemental analysis (CHS) calc (%) for C$_{216}$H$_{260}$Cl$_5$Fe$_{20}$O$_{52}$S$_{20}$V$_8$: C, 43.01; H, 4.35; S, 10.63; found: C, 42.84; H, 4.32; S, 10.41. FT-IR (KBr pellet, cm^{-1}): 3422(m), 2950(s), 1640(w), 1449(s), 1360(w), 1304(w), 1255(s), 989(m), 838(w), and 731(w).

Synthesis of {H[Co$_{20}$(TC4A)$_5$(Cl)$_5$(CH3CH$_2$VO$_4$)$_8$] (+solvents)} (Co$_{20}$V$_8$)

The synthesis of Co$_{20}$V$_8$ is similar to that of Fe$_{20}$V$_8$ except that FeCl$_2$·4H$_2$O was replaced with CoCl$_2$·6H$_2$O (0.4 mmol, 100 mg). Green bulk crystals were obtained with a yield of 62.8 % based on H$_4$TC4A. Elemental analysis (CHS) calc (%) for C$_{216}$H$_{260}$Cl$_5$Co$_{20}$O$_{52}$S$_{20}$V$_8$: C, 42.58; H, 4.30; S, 10.53; found: C, 42.26; H, 4.36; S, 10.93. FT-IR (KBr pellet, cm^{-1}): 3413(m), 2967(s), 1626(w), 1454(s), 1359(w), 1299(w), 1256(s), 833(w), 806(m), and 736(w).

Synthesis of {H[Ni$_{20}$(TC4A)$_5$(Cl)$_5$(CH$_3$CH$_2$VO$_4$)$_8$] (+solvents)} (Ni$_{20}$V$_8$)

The synthesis of Ni$_{20}$V$_8$ is similar to that of Fe$_{20}$V$_8$ except that FeCl$_2$·4H$_2$O was replaced with NiCl$_2$·6H$_2$O (0.40 mmol, 100 mg). Yellow bulk crystals were obtained with a yield of 65.8 % based on H$_4$TC4A. Elemental analysis (CHS) calc (%) for C$_{216}$H$_{260}$Cl$_5$Ni$_{20}$O$_{52}$S$_{20}$V$_8$: C, 42.61; H, 4.30; S, 10.53; found: C, 42.31; H, 4.42; S, 10.23. FT-IR (KBr pellet, cm^{-1}): 3432(m), 2960(s), 1636(w), 1469(s), 1362(w), 1318(w), 1260(s), 838(w), 810(m), and 738(w).

Note: Except for the bulk samples used for thermogravimetric (TG) and powder X-ray diffraction (PXRD), the other samples were used after full drying according to the TGA analysis.

Single crystal X-ray diffraction

The intensity data for Fe$_{20}$V$_8$, Co$_{20}$V$_8$, and Ni$_{20}$V$_8$ were collected on a Bruker D8 QUEST system with Mo-Kα radiation (λ = 0.71073 Å) at 150 K. The crystal structures were solved using direct methods with full-matrix least squares on F^2 (*ShelXT-2014*) and refined with *ShelXL-2019*.[2] The M$_{20}$V$_8$ structures were refined in the $I4$ space group as an inversion twin. All non-hydrogen atoms were refined anisotropically, except for some solvent molecules and disordered parts. The hydrogen atoms of the organic ligands were theoretically generated on specific atoms and refined isotropically with fixed thermal factors. The diffraction data were treated using the "*SQUEEZE*" method as implemented in *PLATON* to subtract the contribution of disordered solvent molecules that cannot be modeled.[3] The solvent molecules that cannot modeled were directly incorporated into the molecular formula and evaluated with *SQUEEZE* and TGA. CCDC numbers 2434503 (Fe$_{20}$V$_8$), 2434504 (Co$_{20}$V$_8$), and 2434505 (Ni$_{20}$V$_8$) contain the supplementary crystallographic data for this paper, which are available free from the Cambridge Crystallography Data Centre (CCDC).

The photothermal experiment in the solid state

The photothermal conversion experiment in the solid state was performed under the illumination of a 520 nm lamp with a power of 0.4 W cm^{-2}. The dry sample (30 mg) was placed on a quartz flake and piled in a 1 cm^2 circle for analysis. The distance between the sample and the lamp was fixed at 10 cm. The test conditions were maintained at approximately 20 °C and 30 % humidity. The sample temperature was

recorded by FL-IR infrared thermography.

The photothermal experiment in the solution

The dry sample was dispersed in $CHCl_3$, and 0.5 mL of the solution was investigated under 520 nm lamp illumination. The sample temperature was recorded by FL-IR infrared thermography.

Photothermal catalysis

The catalyst $M_{20}V_8$ (0.002 mmol), organic sulfide (0.2 mmol), C_9H_{12} (Mesitylene), 30% H_2O_2 (0.4 mmol), and EtOH (5 ml) were introduced into a quartz tube with stirring and subsequently illuminated using a CEL-LED100 LED lamp with a wavelength of 520 nm. Samples of the reaction solution were collected every 0.5 hours. The reaction products were analyzed and quantified using a GC-7920 gas chromatograph equipped with a SE-54 capillary column. The injection port temperature was maintained at 200 °C, the column temperature at 80 °C, and the FID detector at 240 °C. Under these conditions, the retention times for EtOH, C_9H_{12}, MPS, and $MPSO_2$ in the catalytic system were 3.404, 7.676, 10.188, and 15.575 min, respectively. The internal standard method (C_9H_{12}) was employed to calculate sulfide concentration. The conversion rate of the substrate in the reaction solution can be expressed as follows:

$$1 - \frac{S^1_{substrate} \big/ S^1_{C_9H_{12}}}{S^0_{substrate} \big/ S^0_{C_9H_{12}}}$$

Caution: It is imperative to exercise caution when handling mustard gas due to its potential toxicity during experimental procedures. Following the experiment, the waste liquid was appropriately treated.

Determine the solvent molecules in $Fe_{20}V_8$:

The residual electron density of $Fe_{20}V_8$ was treated as a diffuse contribution using the SQUEEZE program. *PLATON/SQUEEZE* gives 700 electrons/unit cell for the voids of $Fe_{20}V_8$, which are occupied by solvents (DMF and or C_2H_5OH). Therefore, the electron densities can be tentatively modeled as 16 DMF (40 e⁻) and 2 C_2H_5OH (26 e⁻) molecules per unit cell. As there are two formula units in one cell (Z = 2), DMF is approximately 12 (incorporating 4 DMF structurally confirmed) and C_2H_5OH is 1 for each formula. The *TENTATIVE* formula for $Fe_{20}V_8$ is $[HFe_{20}(TC4A)_5(Cl)_5(CH_3CH_2VO_4)_8]$ $(DMF)_{12}$ (C_2H_5OH)

\# SQUEEZE RESULTS (APPEND TO CIF)
\# Note: Data are Listed for all Voids in the P1 Unit Cell
\# i.e. Centre of Gravity, Solvent Accessible Volume,
\# Recovered number of Electrons in the Void and
\# Details about the Squeezed Material
loop_
  _platon_squeeze_void_nr
  _platon_squeeze_void_average_x
  _platon_squeeze_void_average_y
  _platon_squeeze_void_average_z
  _platon_squeeze_void_volume
  _platon_squeeze_void_count_electrons
  _platon_squeeze_void_content

nr	average_x	average_y	average_z	volume	count_electrons	content
1	-0.001	-0.001	0.428	2117	334	''*
2	-0.208	0.499	0.928	2117	334	''*
3	0.147	0.700	0.244	12	4	''
4	0.200	0.353	0.744	12	4	''
5	0.300	0.147	0.244	12	4	''
6	0.353	0.800	0.744	12	4	''
7	0.647	0.200	0.744	12	4	''
8	0.700	0.853	0.244	12	4	''
9	0.800	0.647	0.744	12	4	''
10	0.853	0.300	0.244	12	4	''

_platon_squeeze_details
* Possibly occupied by 16 DMF and 2 C_2H_5OH molecules.

Determine the solvent molecules in $Co_{20}V_8$:

The residual electron density of $Co_{20}V_8$ was treated as diffuse contributions using the program *SQUEEZE*. *PLATON/SQUEEZE* gives 192 electrons/unit cell for the voids of $Co_{20}V_8$, which are occupied by solvents (DMF and or C_2H_5OH). Therefore, the electron densities can be tentatively modeled as 6 C_2H_5OH (26 e$^-$) molecules per unit cell. As there are two formula units in one cell (Z =2), DMF is approximately 12 (12 DMF structurally confirmed) and C_2H_5OH is 4 (incorporating 1 C_2H_5OH structurally confirmed) for each formula. The *TENTATIVE* formula for $Co_{20}V_8$ is $[HCo_{20}(TC4A)_5(Cl)_5(CH_3CH_2VO_4)_8] (DMF)_{12} (C_2H_5OH)_4$

```
# SQUEEZE RESULTS (APPEND TO CIF)
# Note: Data are Listed for all Voids in the P1 Unit Cell
# i.e. Centre of Gravity, Solvent Accessible Volume,
# Recovered number of Electrons in the Void and
# Details about the Squeezed Material
loop_
  _platon_squeeze_void_nr
  _platon_squeeze_void_average_x
  _platon_squeeze_void_average_y
  _platon_squeeze_void_average_z
  _platon_squeeze_void_volume
  _platon_squeeze_void_count_electrons
  _platon_squeeze_void_content
```

1	0.000	0.000	0.487	864	80	''*
2	0.017	0.260	0.838	44	4	''
3	-0.017	0.740	0.838	44	4	''
4	0.240	0.516	0.338	44	4	''
5	0.500	0.500	0.987	864	80	''*
6	0.260	0.983	0.838	44	4	''
7	0.483	0.240	0.338	44	4	''
8	0.516	0.760	0.338	44	4	''
9	0.740	0.016	0.838	44	4	''
10	0.760	0.483	0.338	44	4	''

```
_platon_squeeze_details
```
* Possibly occupied by 6 C_2H_5OH molecules.

Determine the solvent molecules in $Ni_{20}V_8$:

The residual electron density of $Ni_{20}V_8$ was treated as diffuse contributions using the program *SQUEEZE. PLATON/SQUEEZE* gives 268 electrons/unit cell for the voids of $Ni_{20}V_8$, which are occupied by solvents (DMF and or C_2H_5OH). So the electron densities can tentatively be modeled as 8 C_2H_5OH (26 e$^-$) molecules per unit cell. As there are two formula units in one cell (Z =2), DMF is approximately 12 (12 DMF structurally confirmed) and C_2H_5OH is 5 (incorporating 1 C_2H_5OH structurally confirmed) for each formula. The *TENTATIVE* formula for $Ni_{20}V_8$ is $[HNi_{20}(TC4A)_5(Cl)_5(CH_3CH_2VO_4)_8]$ $(DMF)_{12}$ $(C_2H_5OH)_5$

SQUEEZE RESULTS (APPEND TO CIF)
Note: Data are Listed for all Voids in the P1 Unit Cell
i.e. Centre of Gravity, Solvent Accessible Volume,
Recovered number of Electrons in the Void and
Details about the Squeezed Material
loop_
  _platon_squeeze_void_nr
  _platon_squeeze_void_average_x
  _platon_squeeze_void_average_y
  _platon_squeeze_void_average_z
  _platon_squeeze_void_volume
  _platon_squeeze_void_count_electrons
  _platon_squeeze_void_content

1	0.000	0.000	0.497	1021	118 ' '*
2	0.035	0.746	0.840	29	4 ' '
3	0.500	0.500	0.997	1021	118 ' '*
4	0.246	0.465	0.340	29	4 ' '
5	0.254	0.035	0.840	29	4 ' '
6	0.465	0.754	0.340	29	4 ' '
7	0.535	0.246	0.340	29	4 ' '
8	0.746	0.965	0.840	29	4 ' '
9	0.754	0.535	0.340	29	4 ' '
10	0.965	0.254	0.840	29	4 ' '

_platon_squeeze_details
* Possibly occupied by 8 C_2H_5OH molecules.
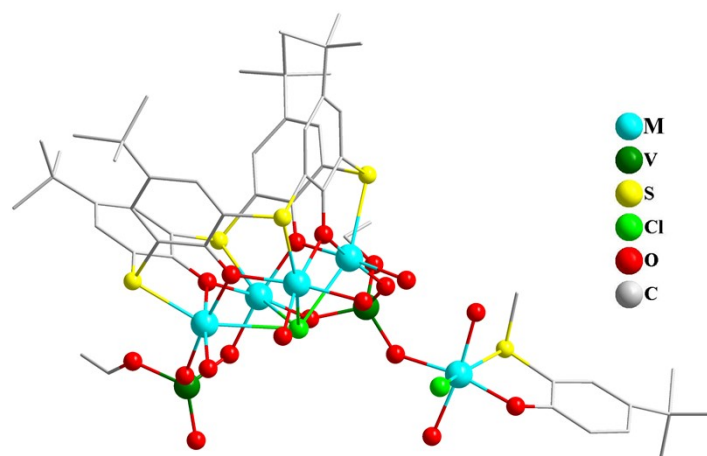
Figures

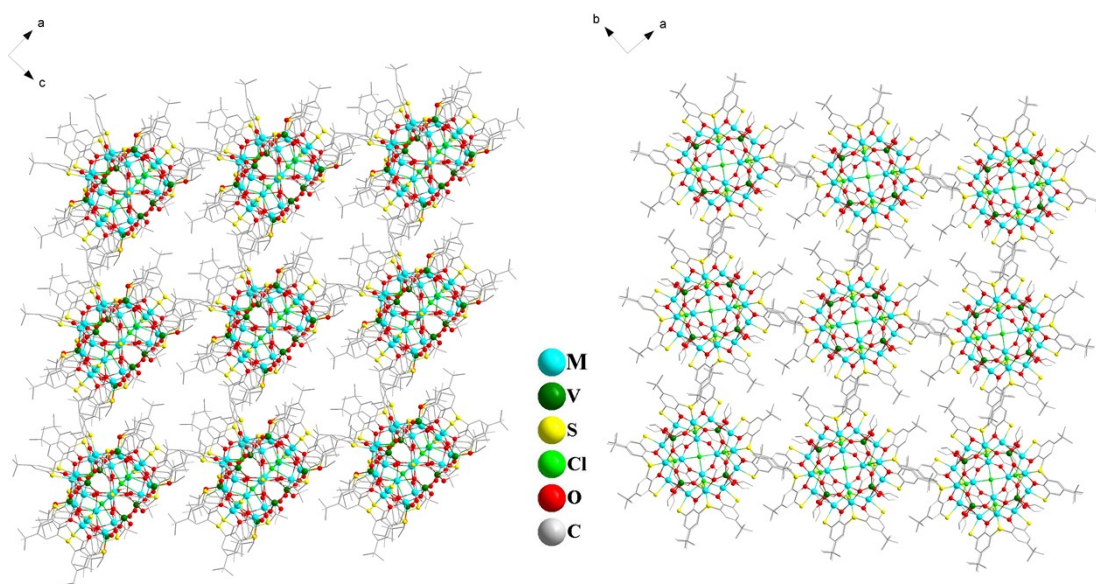**Fig. S1** The asymmetric unit of $M_{20}V_8$.

Fig. S2 Packing diagrams of $M_{20}V_8$ cages along the b (left) and c (right) axes.
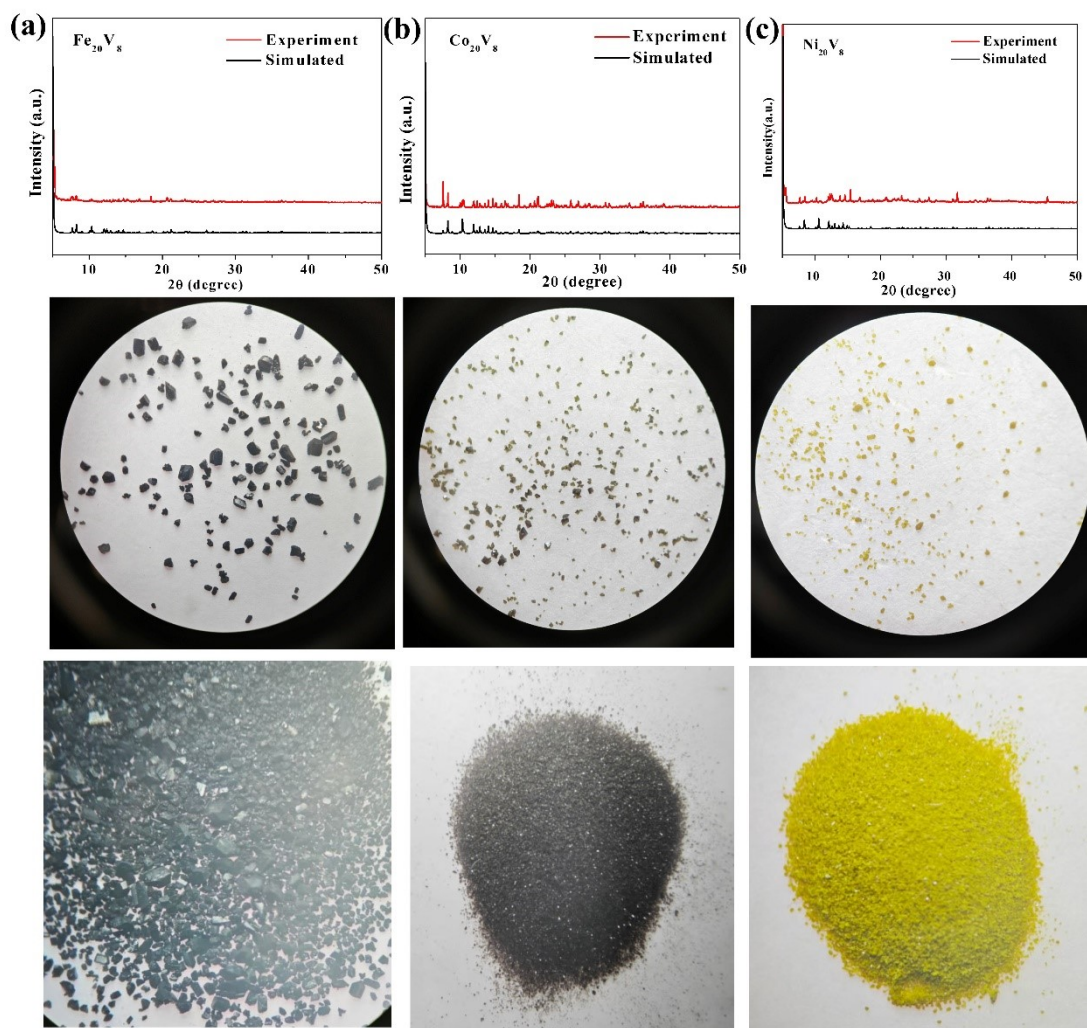
Fig. S3 PXRD patterns (top) and corresponding crystal images (bottom) of (a) $Fe_{20}V_8$, (b) $Co_{20}V_8$, and (c) $Ni_{20}V_8$.

The powder X-ray diffraction (PXRD) patterns of $M_{20}V_8$ matched well with the simulated patterns derived from the single crystal, indicating their high crystallinity and purity.
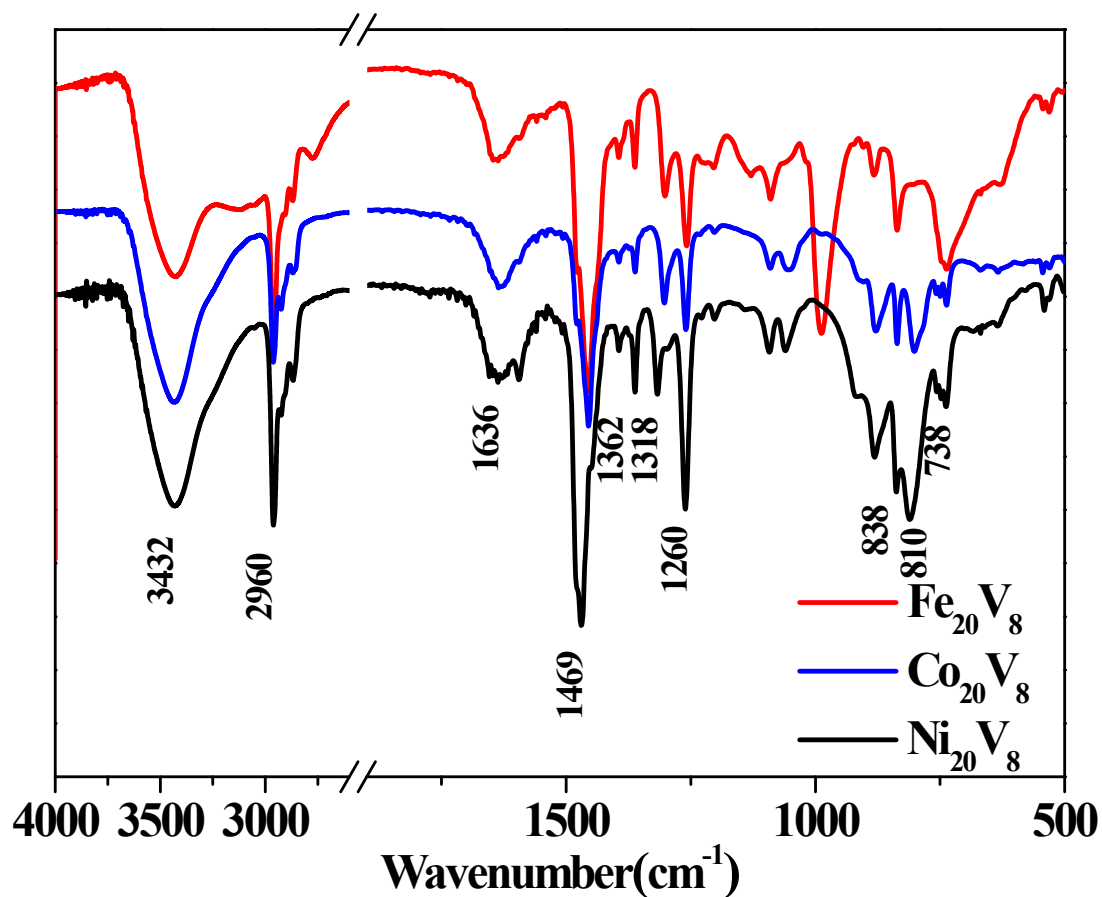
Fig. S4 FT-IR spectra of $Fe_{20}V_8$, $Co_{20}V_8$, and $Ni_{20}V_8$.

The peak at 2960 cm^{-1} was attributed to the tert-butyl group. The characteristic signals at 1636 cm^{-1} and 1469 cm^{-1} are assigned to the benzene ring of TC4A. The C-O stretching vibrations were observed at 1318 cm^{-1} and 1260 cm^{-1}. The peaks at 838 cm^{-1}, 810 cm^{-1}, and 738 cm^{-1} are related to the vibrations of V-O.
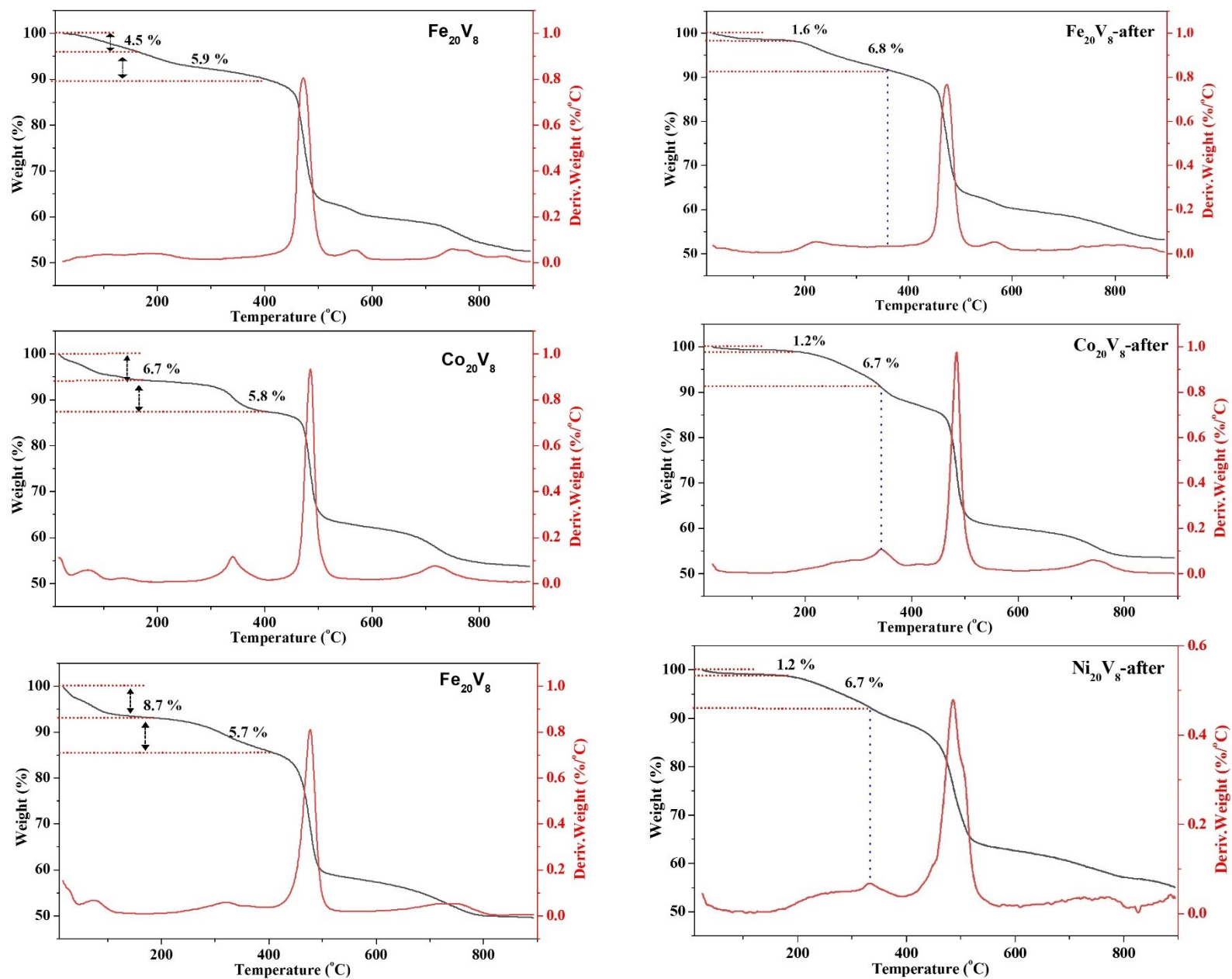
Fig. S5 TGA curves of (a) $Fe_{20}V_8$, (b) $Co_{20}V_8$, and (c) $Ni_{20}V_8$ before (left) and after (right) photothermal conversion (in N_2 with a heating rate of 10 °C/min).

Before: TGA of the three samples in the crystal form was conducted from room temperature to 900 °C. The three samples continuously lost weight from room temperature to 200 °C. The weight loss percentages were 4.5 %, 6.7%, and 8.7% for $Fe_{20}V_8$, $Co_{20}V_8$, and $Ni_{20}V_8$, respectively. These values were all less than the theoretical weight loss values of 13.28%, 14.83%, and 15.38%, respectively, indicating that the samples are prone to losing some crystalline solvents at room temperature. The weight loss between 200 and 400 °C (5.7%-5.9%) can be attributed to the loss of the ethyl group in the vanadate esters (eight per cluster) and Cl coordinated to metal ions at bottom of PSBUs (five per cluster). The three samples rapidly lost weight at approximately 480 °C, corresponding to the decomposition of the molecular skeleton of the clusters and calixarene ligands, accompanied by distinct exothermic peaks. The thermogravimetric residue of the three samples was approximately 50% and remained constant.

Note In the course of handling the prepared crystal samples, we employed ethanol cleaning, which may have resulted in the exchange of some DMF molecules within the lattice. Consequently, in the thermogravimetric analysis (TGA) experiment, the evaporation of the solvents led to a thermogravimetric test value for the solvent that is lower than the solvent value determined by single-crystal diffraction and SQUEEZE. Based on the solvent components (DMF and Ethanol) and the findings from the TGA, all other bulk samples used for investigation, with the exception of those subjected to the PXRD test, were further vacuum-dried at 150 °C for 6 hours.

After: TGA of the samples after photothermal conversion was conducted from room temperature to 900 °C. The three samples lost a small amount of weight (below 2%) from room temperature to 200 °C, corresponding to the adsorption of species in air. Further weight loss take place in the range of 200-400 °C with values of 6.8 %, 6.7%, and 6.7 % for $Fe_{20}V_8$, $Co_{20}V_8$, and $Ni_{20}V_8$, respectively, which can be assigned to loss of the ethyl group and coordinated Cl. The three samples rapidly lost weight at approximately 480 °C, corresponding to the decomposition of the molecular skeleton of the clusters and calixarene ligands, also accompanied by distinct exothermic peaks. TGA of the samples before and after the photothermal reaction revealed that the molecular cluster framework of the samples exhibited thermal stability. Furthermore, the framework stability was preserved even after exposure to a maximum photothermal temperature of 210 °C.
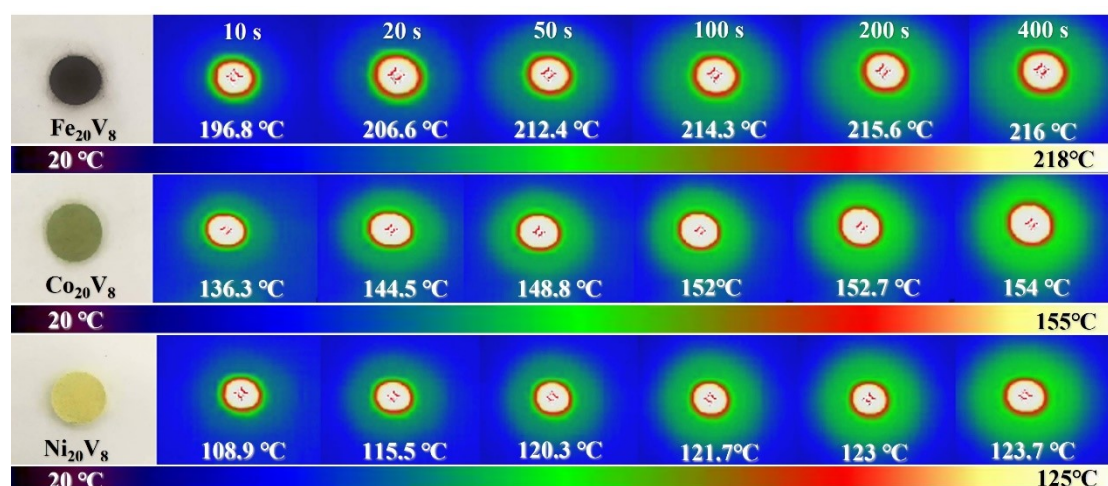
Fig. S6 Thermal images of $Fe_{20}V_8$, $Co_{20}V_8$, and $Ni_{20}V_8$ in the solid state at different irradiation times.
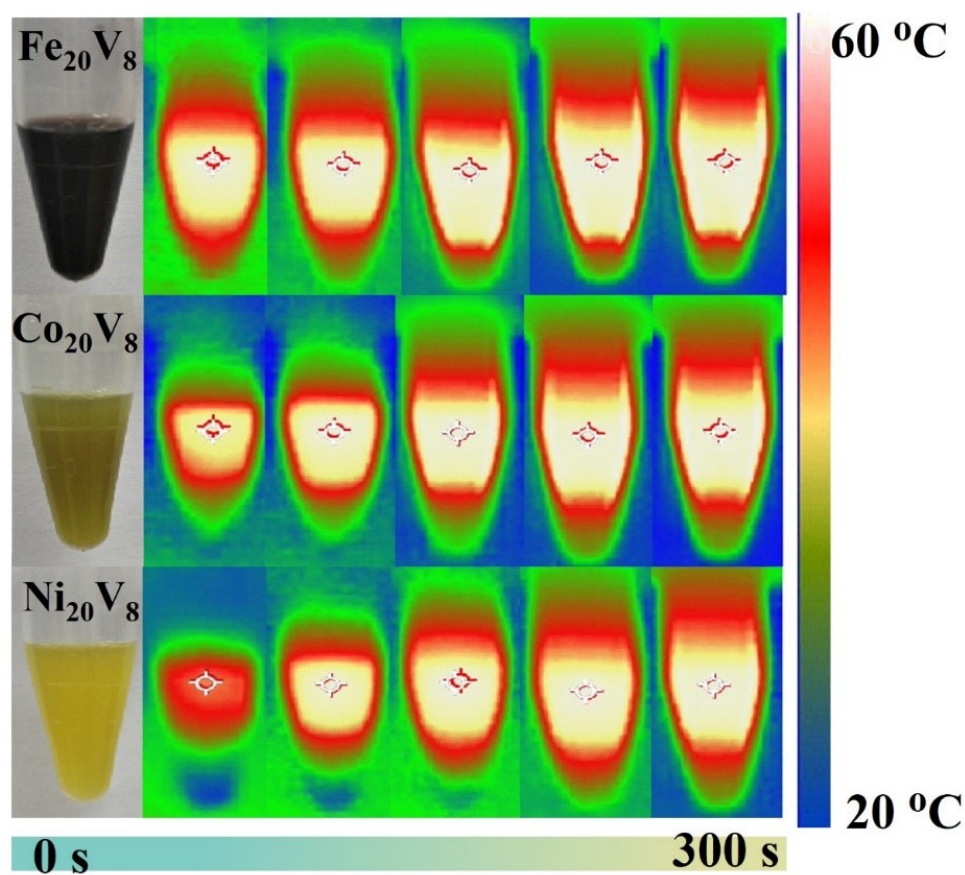

Fig. S7 Thermal images of $Fe_{20}V_8$, $Co_{20}V_8$, and $Ni_{20}V_8$ in $CHCl_3$ at different irradiation times.
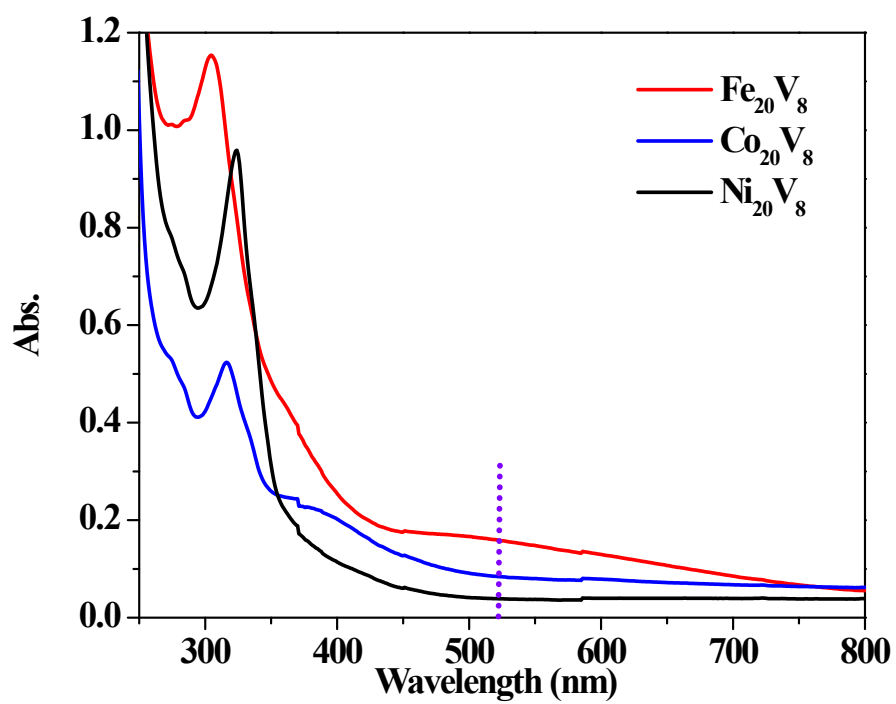
Fig. S8 UV-Vis absorption spectra of $Fe_{20}V_8$, $Co_{20}V_8$, and $Ni_{20}V_8$ in $CHCl_3$ at a concentration of 10.0 μmol/L.
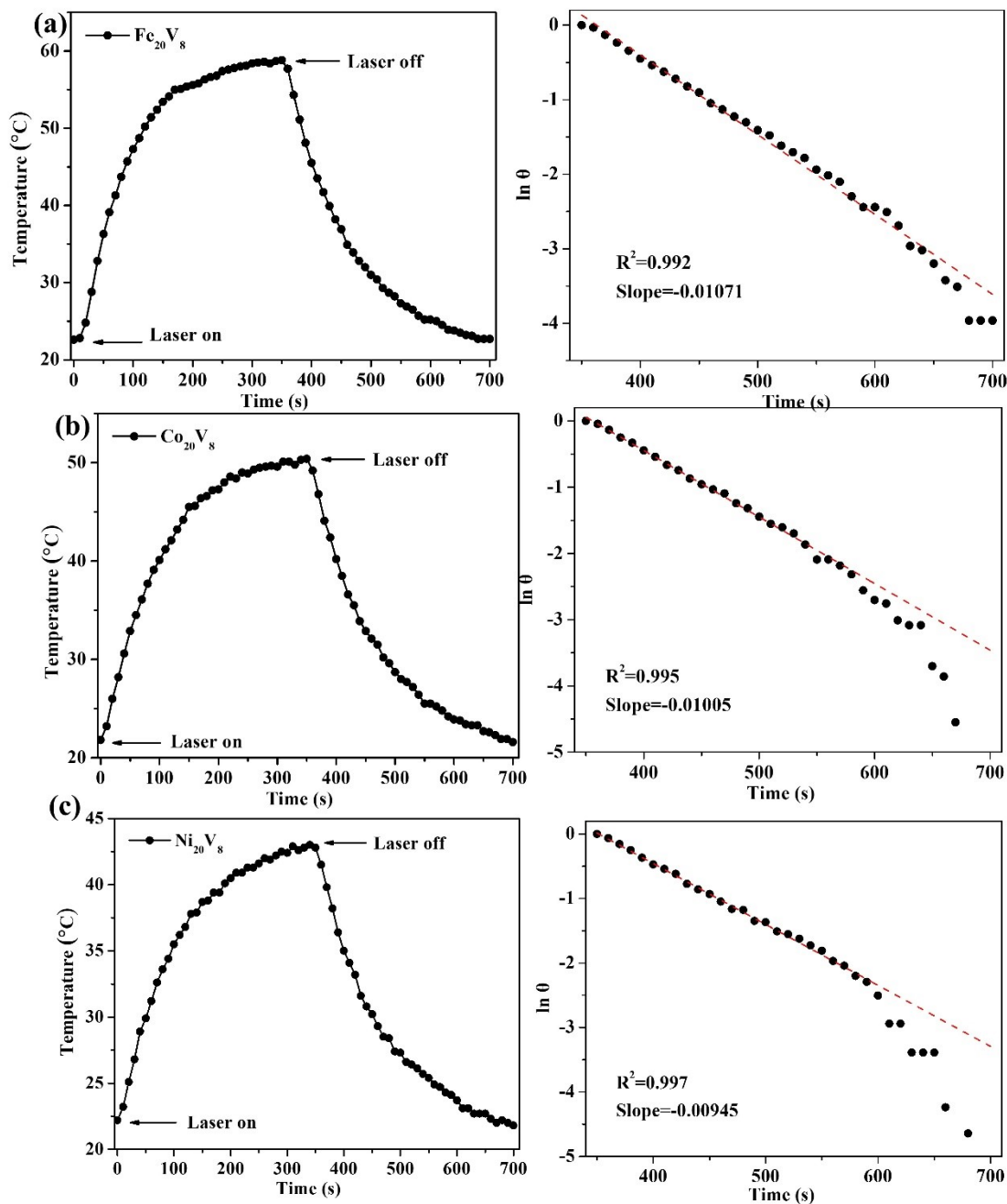
Fig. S9 Amplified the first on-off cycle and corresponding linear fitting of $\ln\theta$-T for $Fe_{20}V_8$ (a), $Co_{20}V_8$(b), and $Ni_{20}V_8$(c), respectively.

The $CHCl_3$ solution of $Fe_{20}V_8$ (1 mmol L^{-1}) was placed under the lamp (520 nm, 0.4 W cm^{-2}) until a steady-state temperature was reached. Subsequently, the lamp was turned off, and the decrease in the temperature of the solution was recorded to measure the rate of heat transfer from the $Fe_{20}V_8$ solution to the environment. The photothermal conversion efficiency of the $Fe_{20}V_8$ was calculated as follows:

$$\sum_i m_i C_{pi}\frac{dT}{dt} = Q_s - Q_{loss} \quad (1)$$

where m (0.74 g) and C_p (1.189 J g^{-1} °C^{-1}) are the mass and heat capacity of CHCl$_3$, respectively. Q_s is the photothermal heat energy input by irradiating I, and Q_{loss} is thermal energy lost to the surroundings. When the temperature is at its maximum, the system is balanced.

$$Q_s = Q_{loss} = hs\Delta T_{max} \quad (2)$$

where h is the heat transfer coefficient, s is the surface area of the container, and ΔT_{max} is the maximum temperature change. The η is calculated from the following equations:

$$\eta = \dfrac{hs\Delta T_{max}}{I(1 - 10^{-A_{520}})} \quad (3)$$

$$hs = \dfrac{\sum_i m_i C_{pi}}{\tau_s} \quad (4)$$

$$\tau_s = \dfrac{-t}{\ln\theta} \quad (5)$$

$$\theta = \dfrac{T_{amb} - T}{T_{amb} - T_{max}} \quad (6)$$

where I is the laser power (0.4 W cm^{-2}), A_{520} is the absorbance of the samples at 520 nm, t is the time of the cooling process, and T_{amb} is 20 °C. The η of the CHCl$_3$ solution of Fe$_{20}$V$_8$ at a concentration of 1 mmol L^{-1} under 520 nm laser irradiation was calculated using the above equations.

Using the cooling process data from the first cycle, the calculation is as follows:

The η of the CHCl$_3$ solution of Fe$_{20}$V$_8$ at a concentration of 1 mmol L^{-1} under 520 nm laser irradiation was calculated according to Equation (1-6).

A fitting linear of $\ln\theta$-T with a slope of -0.01071, by which τ_s was calculated as 93.37 (slope= -1 / τ_s). $\Sigma mC_p = \rho(CHCl_3)\cdot V(CHCl_3)\cdot Cp(CHCl_3) = 0.5$ mL × 1.48 g mL^{-} × 1.189 J g^{-1} °C^{-1} = 0.88 J °C^{-1}. Therefore, hs = 0.88 / 93.37 = 9.42 × 10^{-3} J·°C^{-1}·S^{-1}. ΔT_{sample} = 36.8 °C. $\Delta T_{solvent}$ = 1°C. A-Fe$_{20}$V$_8$ = 0.1599 × 100 = 15.99

Eventually, η-Fe$_{20}$V$_8$ = 9.42 × 10^{-3} × (36.8 - 1) / [0.4 × (1 - 10$^{-15.99}$)] = 84.34 %.

A fitting linear of $\ln\theta$-T with a slope of -0.01005, by which τ_s was calculated as 99.5 (slope= -1 / τ_s). $\Sigma mC_p = \rho(CHCl_3)\cdot V(CHCl_3)\cdot Cp(CHCl_3) = 0.5$ mL × 1.48 g mL^{-} ×

1.189 J g^{-1} $^{\circ}$C^{-1} = 0.88 J $^{\circ}$C^{-1}. Therefore, hs = 0.88 / 99.5 = 8.84× 10^{-3} J·$^{\circ}$C^{-1}·S^{-1}. ΔT$_{sample}$ = 28.4°C. ΔT$_{solvent}$ = 1°C. A-Co$_{20}$V$_8$ = 0.0848 × 100 = 8.48

Eventually, η-Co$_{20}$V$_8$ = 8.84 × 10^{-3} × (28.4 - 1) / [0.4 × (1 - 10$^{-8.48}$)] = 60.55 %.

A fitting linear of lnθ-T with a slope of -0.00945, by which τ_s was calculated as 105.82 (slope= -1 / τ_s). ΣmC$_p$ = ρ(CHCl$_3$)·V(CHCl$_3$)·Cp(CHCl$_3$) = 0.5 mL × 1.48 g mL$^-$ × 1.189 J g^{-1} $^{\circ}$C^{-1} = 0.88 J $^{\circ}$C^{-1}. Therefore, hs = 0.88 / 105.82= 8.31× 10^{-3} J·$^{\circ}$C^{-1}·S^{-1}. ΔT$_{sample}$ = 20.8°C. ΔT$_{solvent}$ = 1°C. A-Ni$_{20}$V$_8$ = 0.039 × 100 = 3.90

Eventually, η-Ni$_{20}$V$_8$ = 8.31 × 10^{-3} × (20.8 - 1) / [0.4 × (1 - 10$^{-3.9}$)] = 41.16 %.

By fitting the data of the other five cycle cooling processes, η-Fe$_{20}$V$_8$ = 85.87 ±2.03 %, η-Co$_{20}$V$_8$ = 60.67 ±1.06 %, and η-Ni$_{20}$V$_8$ = 40.93±0.15 % were obtained.
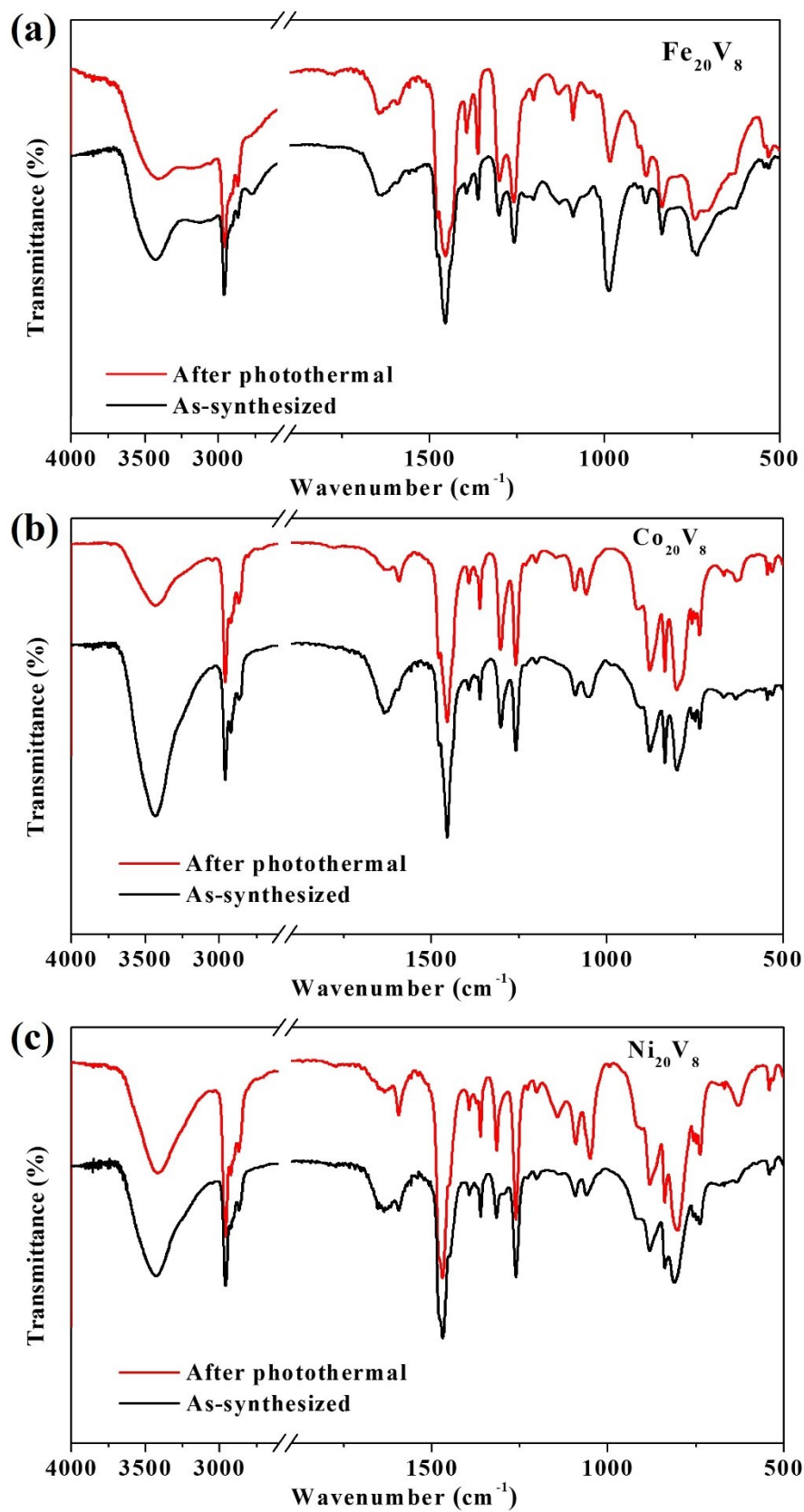
Fig. S10 FT-IR spectra of (a) $Fe_{20}V_8$, (b) $Co_{20}V_8$, and (c) $Ni_{20}V_8$ before and after the photothermal conversion.

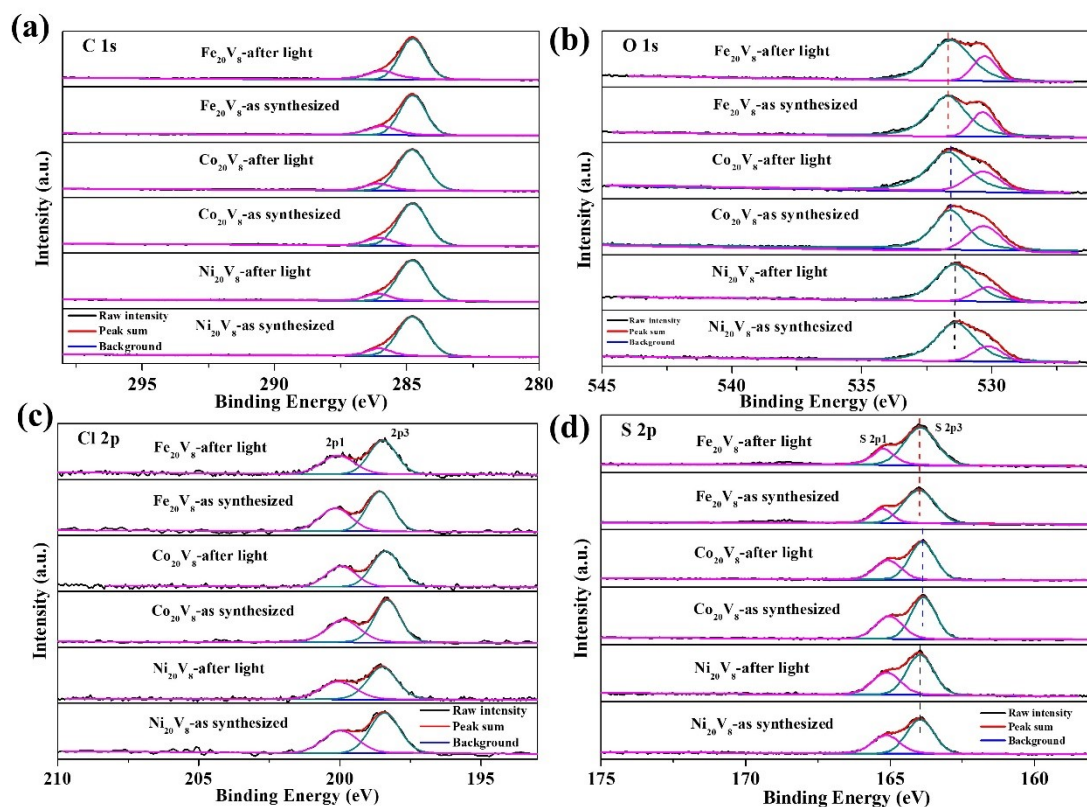**Fig. S11** High-resolution XPS spectra of $M_{20}V_8$ (M = Fe, Co, Ni) before and after the photothermal conversion. (a) C 1s, (b) O 1s, (c) S 2p, and (d) Cl 2p.

**Table S1** Crystal data and structural refinement parameters for $M_{20}V_8$ (M = Fe, Co, Ni)

Complex	$Fe_{20}V_8$	$Co_{20}V_8$	$Ni_{20}V_8$
Formula	$C_{254}H_{351}Cl_5Fe_{20}N_{12}O_{65}S_{20}V_8$	$C_{260}H_{369}Cl_5Co_{20}N_{12}O_{68}S_{20}V_8$	$C_{262}H_{375}Cl_5Ni_{20}N_{12}O_{69}S_{20}V_8$
Formula weight	6955.42	7155.22	7196.89
Crystal system	Tetragonal	Tetragonal	Tetragonal
space group	$I4$(No. 79)	$I4$(No. 79)	$I4$(No. 79)
a (Å)	26.9722(13)	26.857(3)	26.771(2)
b (Å)	26.9722(13)	26.857(3)	26.771(2)
c (Å)	22.8711(14)	23.006(3)	23.0428(19)
α (°)	90	90	90
β (°)	90	90	90
γ (°)	90	90	90
Volume (Å^3)	16638.7(19)	16594(5)	16515(3)
Z	2	2	2
Temperature (K)	150	150	150
Dc (g/cm^3)	1.388	1.432	1.447
μ (mm^{-1})	1.285	1.416	1.559
Reflections collected	94058	77285	75315
Unique data	14257	13959	13127
(R_{int})	0.034	0.059	0.034
GOF on F^2	1.023	1.027	1.014
[a]R_1 [I>2sigma(I)]	0.0459	0.0450	0.0378
[b]wR_2	0.1415	0.1205	0.1068

[a]$R_1 = \Sigma||F_0|-|F_c||/\Sigma|F_0|$; [b]$wR_2 = \{\Sigma[w(F_0{}^2-F_c{}^2)^2]/\Sigma[w(F_0{}^2)^2]\}^{1/2}$.

Table S2 The selected bond lengths (Å) and bond valance calculations (BVS) for $M_{20}V_8$ (M = Fe, Co, Ni)

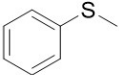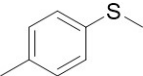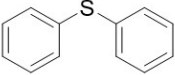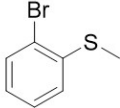| Bond	M = Fe			M = Co			M = Ni		
	Distance	r	Value	Distance	r	Value	Distance	r	Value
M1-O1	2.012(5)	1.734	0.472	2.003(5)	1.692	0.431	1.959(4)	1.654	0.439
M1-O4	2.045(5)	1.734	0.431	1.981(5)	1.692	0.458	1.978(4)	1.654	0.417
M1-O11	2.035(5)	1.734	0.443	2.044(5)	1.692	0.386	1.990(5)	1.654	0.403
M1-O7	2.099(5)	1.734	0.373	2.077(5)	1.692	0.353	2.049(4)	1.654	0.344
M1-S1	2.5663(15)	2.16	0.334	2.517(2)	2.06	0.291	2.446(14)	2.04	0.334
M1-Cl1	2.6246(14)	2.06	0.217	2.612(2)	2.01	0.197	2.649(15)	2.02	0.183
valence			2.270	valence		2.116	valence		2.119
Bond	Distance	r	Value	Distance	r	Value	Distance	r	Value
M2-O2	2.026(5)	1.734	0.454	1.997(6)	1.692	0.439	1.965(4)	1.654	0.431
M2-O1	2.060(5)	1.734	0.414	1.978(5)	1.692	0.462	1.987(4)	1.654	0.407
M2-O6	2.059(4)	1.734	0.415	2.015(5)	1.692	0.418	2.019(4)	1.654	0.373
M2-O8i	2.075(5)	1.734	0.398	2.092(6)	1.692	0.339	2.046(4)	1.654i	0.347
M2-S2	2.562(2)	2.16	0.337	2.508(17)	2.06	0.298	2.467(18)	2.04	0.316
M2-Cl1	2.657(2)	2.06	0.199	2.639(17)	2.01	0.183	2.559(19)	2.02	0.233
valence			2.218	valence		2.138	valence		2.106
Bond	Distance	r	Value	Distance	r	Value	Distance	r	Value
M3-O2	2.029(5)	1.734	0.451	1.987(5)	1.692	0.451	1.967(4)	1.654	0.429
M3-O3	2.049(5)	1.734	0.427	2.000(5)	1.692	0.435	1.981(4)	1.654	0.413
M3-O11i	2.048(5)	1.734	0.428	2.033(6)	1.692	0.398	2.005(5)	1.654	0.387
M3-O7i	2.119(5)	1.734	0.353	2.103(6)	1.692	0.329	2.052(4)	1.654	0.341
M3-S3	2.558(15)	2.16	0.341	2.498(17)	2.06	0.306	2.438(14)	2.04	0.342
M3-Cl1	2.620(14)	2.06	0.220	2.633(17)	2.01	0.185	2.693(15)	2.02	0.162
valence			2.220	valence		2.104	Distance		2.075
Bond	Distance	r	Value	Distance	r	Value	Distance	r	Value
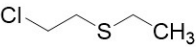
Bond	Distance	r	Value	Distance	r	Value	Distance	r	Value
M4-O10	2.010(6)	1.734	0.474	2.000(7)	1.692	0.435	1.995(5)	1.654	0.398
M4-O3	2.048(5)	1.734	0.428	2.005(7)	1.692	0.429	1.986(5)	1.654	0.408
M4-O12^i	2.054(6)	1.734	0.421	2.011(6)	1.692	0.422	1.980(5)	1.654	0.414
M4-O4	2.064(5)	1.734	0.410	2.013(6)	1.692	0.420	1.987(5)	1.654	0.407
M4-S4	2.555(2)	2.16	0.344	2.488(3)	2.06	0.315	2.424(2)	2.04	0.354
valence			2.077			2.021			1.981
Bond	Distance	r	Value	Distance	r	Value	Distance	r	Value
M5-O8	2.015(5)	1.734	0.468	2.026(5)	1.692	0.405	2.006(4)	1.654	0.386
M5-O5	2.011(4)	1.734	0.473	1.972(5)	1.692	0.469	1.977(4)	1.654	0.418
M5-O5^i	2.045(5)	1.734	0.431	1.992(5)	1.692	0.444	1.961(4)	1.654	0.436
M5-O6^{ii}	2.160(5)	1.734	0.316	2.090(5)	1.692	0.341	2.044(4)	1.654	0.349
M5-S5^i	2.566(2)	2.16	0.334	2.510(2)	2.06	0.296	2.450(16)	2.04	0.330
M5-Cl2	2.663(17)	2.06	0.196	2.663(19)	2.01	0.171	2.665(15)	2.02	0.175
valence			2.218			2.128			2.094
Bond	Distance	r	Value	Distance	r	Value	Distance	r	Value
V1-O7	1.698(5)	1.803	1.328	1.689(6)	1.803	1.361	1.707(4)	1.803	1.296
V1-O6	1.701(5)	1.803	1.317	1.708(5)	1.803	1.293	1.694(5)	1.803	1.343
V1-O8	1.722(5)	1.803	1.245	1.706(5)	1.803	1.300	1.700(4)	1.803	1.321
V1-O9	1.757(5)	1.803	1.132	1.759(6)	1.803	1.126	1.761(5)	1.803	1.120
valence			5.023			5.080			5.080
Bond	Distance	r	Value	Distance	r	Value	Distance	r	Value
V2-O12	1.622(7)	1.803	1.631	1.625(7)	1.803	1.618	1.660(6)	1.803	1.472
V2-O10	1.635(6)	1.803	1.575	1.716(6)	1.803	1.265	1.642(6)	1.803	1.545
V2-O11	1.714(5)	1.803	1.272	1.627(7)	1.803	1.609	1.712(5)	1.803	1.279
V2-O13	1.710(9)	1.803	1.286	1.784(16)	1.803	1.053	1.747(7)	1.803	1.163
valence			5.763			5.545			5.459

Symmetry codes: (i) $x, y, -z+1$; (ii) $-x+1, -y+1, -z+1$; (iii) $-x+1, -y+1, z$

Table S3 Visible-light-driven photocatalytic oxidative desulfurization of methyl phenyl sulfide [a]
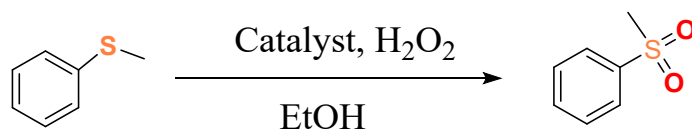
Entry	Catalyst	Oxidant	Reaction condition	Time (h)	Conv. (%)
1	$Fe_{20}V_8$	H_2O_2	520 nm	0.5	70
				1	>99
2	$Co_{20}V_8$	H_2O_2	520 nm	0.5	31
				1	53
3	$Ni_{20}V_8$	H_2O_2	520 nm	0.5	26
				1	36
4	$Fe_{20}V_8$	H_2O_2	Dark	0.5	12
				1	42
5	$Fe_{20}V_8$	H_2O_2	520 nm (controlled 20 °C)	0.5	52
				1	80
6	$M_{20}V_8$	O_2	520 nm	6	trace
7	$M_{20}V_8$	none	520 nm	6	trace

[a] Reaction conditions: substrate: methyl phenyl sulfide (0.2 mmol): H_2O_2 (0.4 mmol) = 1:2, catalyst: 0.002 mmol, solvent: CH_3CH_2OH, light source: 520 nm LED light, internal standard solvent: mesitylene. Room temperature 20 °C.

Table S4 Visible-light-driven photocatalytic oxidative desulfurization of other thioethers substrates [a]

Entry	Substrate	Time (h)	Conv. (%)
1		1	>99
2		1	>99
3		1	>99
4		1	74
		2	>99
5		0.5	>99

[a] Reaction conditions: substrate: thioethers (0.2 mmol): H_2O_2 (0.4 mmol) = 1:2, catalyst: 0.002 mmol, solvent: CH_3CH_2OH, light source: 520 nm LED light, internal standard solvent: mesitylene. The sulfone selective oxidation products were detected
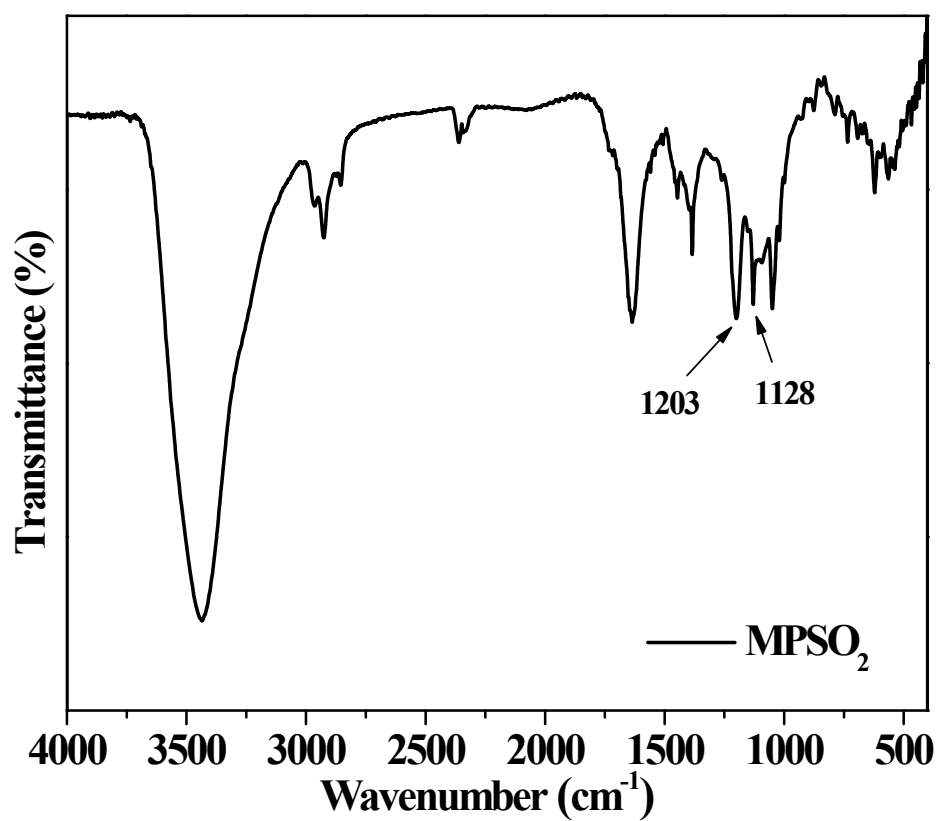
Fig. S12 FT-IR spectrum of the oxidative desulfurization product (methyl phenyl sulfone, MPSO$_2$) of methyl phenyl sulfide.
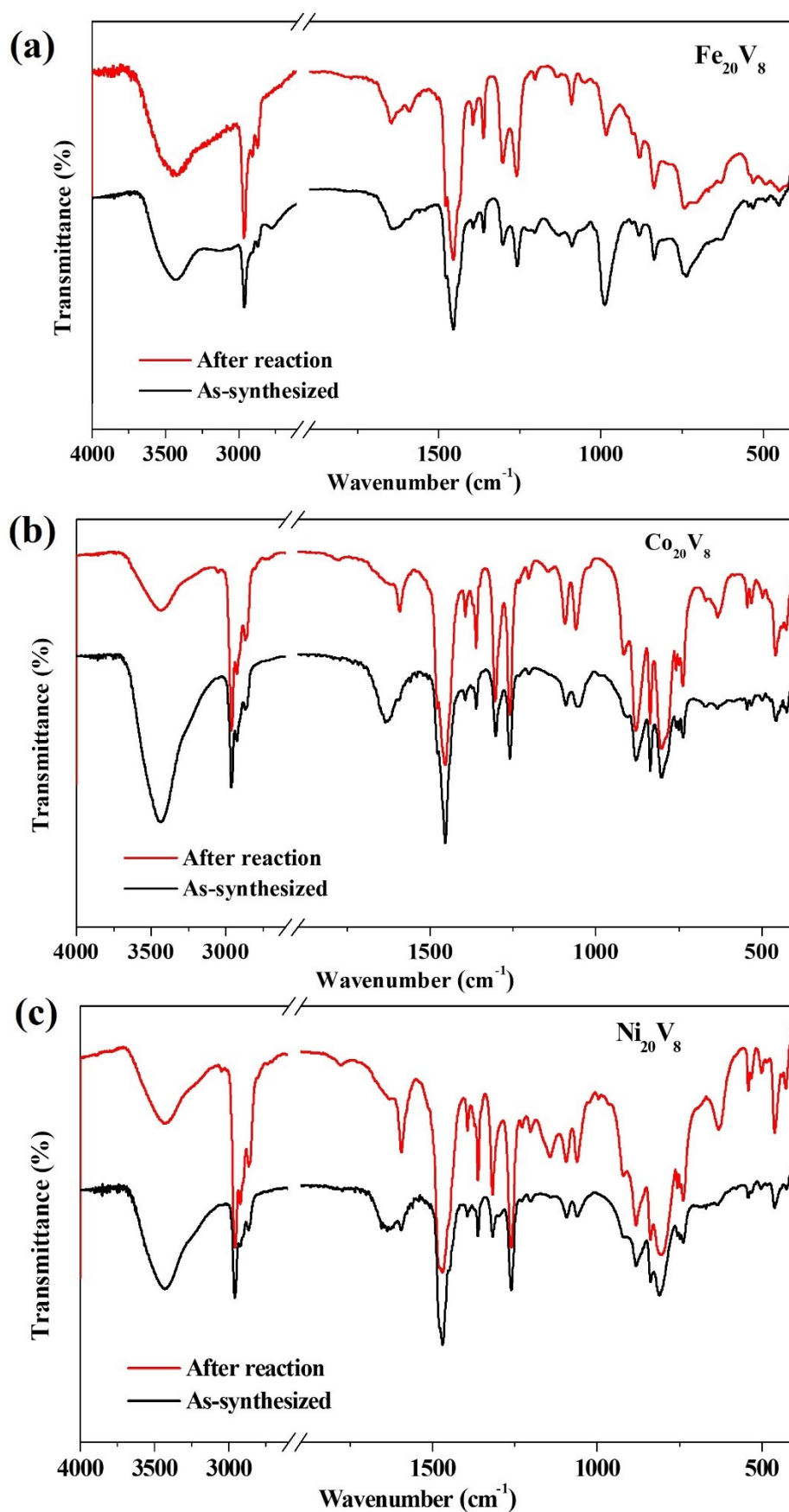
Fig. S13 FT-IR spectra of (a) $Fe_{20}V_8$, (b) $Co_{20}V_8$, and (c) $Ni_{20}V_8$ before and after the photocatalytic reaction.

References

1. N. Iki, C. Kabuto, T. Fukushima, H. Kumagai, H. Takeya, S. Miyanari, T. Miyashi and S. Miyano, *Tetrahedron*, 2000, **56**, 1437-1443.

2. G. M. Sheldrick, *Acta Crystallogr.,* Sect. *A: Found Adv*, 2015, **71**, 3-8.

3. A. L. Spek, *Acta Crystallogr., Sect. C: Struct. Chem.,* 2015, **71**, 9-18.